Positioning of a Reference Electrode in a PEM Fuel Cell

A. A. Kulikovsky[a,b,*,z] and P. Berg[c,*,z]

[a] Forschungszentrum Juelich GmbH, Institute of Energy and Climate Research, IEK-3: Electrochemical Process Engineering, D-52425 Jülich, Germany
[b] Moscow State University, Research Computing Center, 119991 Moscow, Russia
[c] Department of Physics, NTNU, 7491 Trondheim, Norway

We report an analytical solution for the membrane potential in a PEM fuel cell which consist of a half-plane (semi-infinite) anode and a large-area (infinite) cathode. Mathematically, the problem is analogous to the Gouy–Chapman problem for the potential distribution inside the diffuse double layer at a flat metal/electrolyte interface. An expression for the characteristic length l_* of the membrane potential variation in the anode-free domain is derived. This expression suggests a minimum distance $3l_*$ between the anode edge and a reference electrode at which the potential of the reference electrode yields the cathode overpotential in the working domain of the cell.

Electrochemical reactions on either side of a fuel cell are driven by the respective half-cell polarization overpotentials in the electrodes. These overpotentials contain contributions from activation and transport losses; rationalizing these contributions is of utmost importance for better cell design. One of the most popular techniques for measuring the half-cell overpotentials is the reference-electrode method.[1,2]

A reference electrode (RE) measures the electrolyte potential Φ at the place of RE location. This value corresponds to the potential at some point between working electrodes. Knowledge of this potential enables one, in principle, to distinguish between the cathode and anode polarization overpotentials. However, the proper positioning of the RE is not a simple task.

Generally, there are two options for placing the RE. The first option is to embed the RE directly into the membrane (Fig. 1a). This design is relatively easy to realize in polymer electrolyte fuel cells (PEMFCs) using a two-layer membrane with a platinum wire located between the layers[3,4] (Fig. 1a). The bare tip of the wire serves as a reference electrode, while the rest of the wire is insulated from the protons. To provide the RE with hydrogen, a second wire can be embedded close to the RE; application of a DC potential to the wires leads to water electrolysis and hydrogen evolution from the RE surface. Note that this design is more difficult to realize in solid oxide fuel cells (SOFCs), which employ ceramic ion conductors as electrolytes.

A disadvantage of this design is that the exact location of the RE relative to the catalyst layers is difficult to control. Upon pressurizing the two-layer membrane in Fig. 1a, the platinum wire shifts from the exact center position toward one of the electrodes. This makes it challenging to interpret properly the DC signal obtained from the wire tip; the half-cell polarizations can be obtained by means of impedance spectroscopy only.[4]

The second option is to place the RE at one of the electrodes, at a certain distance L_{gap} away from the aligned edges of the working electrodes (Fig. 1b). Calculations of Adler et al.[5] have shown that L_{gap} must be larger than $3l_m$, where l_m is the membrane thickness. At this distance, the inhomogeneities caused by the working electrode edge vanish and Φ is nearly uniform through the membrane depth. In cells with protons as charge carriers, the hydrogen-fed RE has a potential Φ, which corresponds to a membrane potential between the working electrodes. Here and below, we assume that the working anode is grounded and all potentials are measured with respect to the working anode.

The main problem with the design in Fig. 1b is that even a small misalignment δ of the edges of the working electrodes strongly changes the value of Φ at the RE. This problem has been widely discussed in SOFC literature; a number of rather sophisticated cell

and electrode geometries that aim to minimize this effect, have been tested by Winkler et al.[6] and Adler.[7] A straightforward solution for PEMFCs has recently been suggested by Gerteisen[8] who reported a precisely aligned system of working and reference electrodes, made by means of laser ablation cutting.

Another problem is that in a fuel cell with perfectly aligned working electrodes and poorly conductive electrolyte, the value of Φ, as measured by the RE in Fig. 1b, corresponds to a certain, yet unknown point along the y-axis between the working electrodes. Again, the DC signal cannot be correctly interpreted and the determination of the anode and cathode overpotentials requires impedance spectroscopy. The system in Fig. 1b and its variants have been widely employed in SOFC impedance studies.[5–7,9] A review of RE geometries in SOFCs has been reported by Rutman and Riess.[9]

Ohs et al.[4] placed a RE inside a 15-mm circular gap in the cathode catalyst layer of a PEMFC (Fig. 2). However, an attempt to measure the cathode polarization with this system failed: under all cell current densities, the RE potential appeared to be close to zero. Numerical calculations[4] have shown that the membrane potential Φ at the RE is close to the potential of the *working anode*, i.e., $\Phi \simeq 0$. To explain this effect, calculations[4] were performed, assuming a very low in-plane proton conductivity of the membrane.
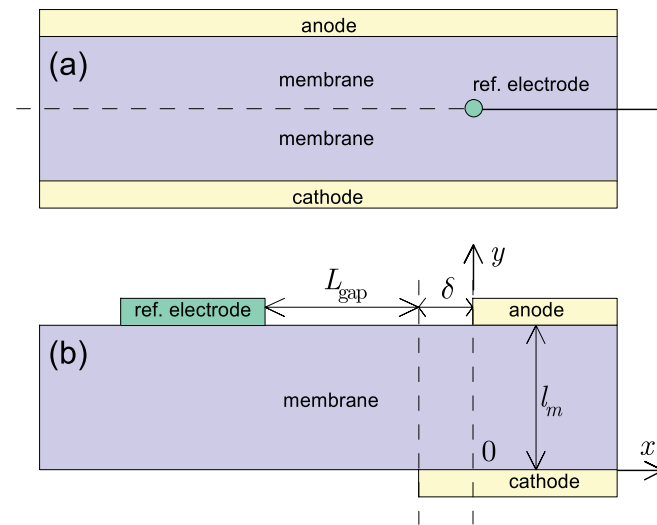

Figure 1. (Not to scale) Conventional variants of positioning the reference electrode (RE) in a fuel cell. (a) An insulated Pt wire with a bare head is embedded between two layers of membrane. (b) A planar RE is placed at the distance $L_{gap} \simeq 3l_m$ away from the edge of the working anode and cathode. A small misalignment δ can significantly distort the signal from the RE.

*Electrochemical Society Active Member.
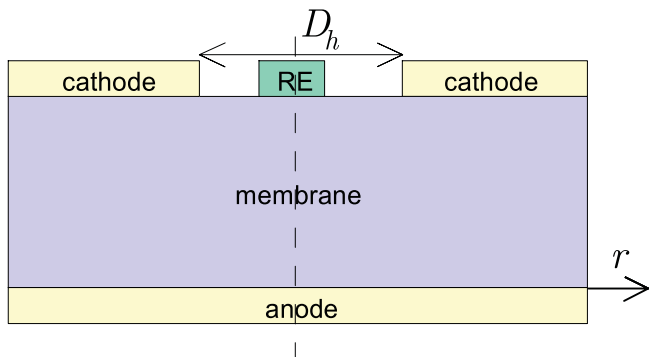zE-mail: A.Kulikovsky@fz-juelich.de; peter.berg@ntnu.no

Figure 2. Schematic of the reference-electrode placement in experiments by Ohs et al.[4] Note the radial symmetry of the system with a hole in the cathode catalyst layer of diameter $D_h = 1.5$ cm.

Below, we will show that this effect arises, in fact, from the very large exchange current density of the anodic hydrogen oxidation reaction (HOR). Even if the membrane in-plane conductivity is high, the length scale for the decay in the membrane potential at the edge of the cathode catalyst layer (Fig. 2) is small, about a hundred micrometers. In other words, in PEMFCs and HT-PEMFCs with a large HOR exchange current density, the potential of the membrane, and hence of the reference electrode in Fig. 2, is close to zero. Thus, measuring the cathode polarization, which is of primary interest for these cells, by means of a RE located at the cathode side, is not possible. However, this polarization can be measured by placing the RE on the other side of the cell, as discussed below.

Modeling studies of fuel cells that include a RE have been based on two-dimensional simulations of the membrane potential in a plane perpendicular to the working and reference electrodes.[4,7,10] Numerical calculations, however, provide neither parametric dependencies nor characteristic scales for the variation of Φ in such systems. Below, we solve the problem for a PEMFC with a single-edge (semi-infinite) working anode and an infinite working cathode, exhibited in Fig. 3. An analytical solution for the shape of $\Phi(x)$ in this system is obtained and the characteristic length scale l_* of Φ variations along the x-axis is derived. We show that a RE placed at a distance $L_{gap} \gtrsim 3l_*$ from the edge of the working anode, yields a potential which *is equal to the cathode overpotential in the working cell area*. Lastly, it is worth mentioning that the basic schematic of the cell considered in this work is also realized in cells with catalyzed strips on the anode side.[11]
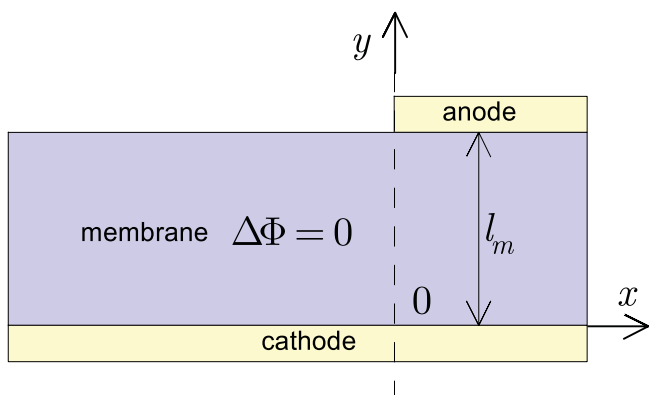

Figure 3. (Not to scale) Schematic of the membrane-electrode assembly with a single anode edge, located at $x = 0$ above the infinite cathode.

Model and Basic Equations

Consider a PEM fuel cell with an electrode structure and a system of coordinates as shown in Fig. 3. In the following, the domains $x < 0$ and $x > 0$ will be referred to as the anode–free and the working domain, respectively. The derivation of the basic equations outlined below, is similar in spirit to that described in Ref. 12.

In the absence of a pressure gradient inside a well-humidified membrane, the key variable determining the distribution of the local current inside the membrane, is the membrane potential Φ. Since no current is produced or consumed inside the membrane, Φ must fulfill the Laplace equation

$$\frac{\partial^2 \Phi}{\partial x^2} + \frac{\partial^2 \Phi}{\partial y^2} = 0. \quad [1]$$

This equation implicitly states that the proton conductivity is constant across the membrane, which is a reasonable assumption under sufficient humidification. Approximating the second derivative along the y-axis by the difference of local proton currents entering and leaving the membrane, Eq. 1 can be reduced to[13]

$$\frac{d^2 \Phi}{dx^2} = \frac{j_c - j_a}{\sigma_m l_m}, \quad [2]$$

where σ_m is the membrane proton conductivity, l_m the membrane thickness, and j_a and j_c are the proton current densities at the anode and cathode side of the membrane, respectively. Further, j_a and j_c are assumed to obey the Butler–Volmer kinetics

$$j_a = 2 j_{hy} \sinh\left(\frac{\eta_a}{b_{hy}}\right), \quad [3]$$

$$j_c = 2 j_{ox} \sinh\left(-\frac{\eta_c}{b_{ox}}\right). \quad [4]$$

Here, j_{hy} and j_{ox} are the superficial exchange current densities of the anode catalyst layer (ACL) and of the cathode catalyst layer (CCL), respectively, η_a and η_c are the local electrode overpotentials, and b_{hy} and b_{ox} are the corresponding Tafel slopes. Note that the dependencies on the reactant concentrations are included in j_{hy} and j_{ox} since we assume that the transport losses are small (see discussion further below).

The anode and cathode overpotentials are given by

$$\eta_a = \phi_a - \Phi - E_{HOR}^{eq}, \quad [5]$$

$$\eta_c = \phi_c - \Phi - E_{ORR}^{eq}, \quad [6]$$

where ϕ_a and ϕ_c are the electrode (carbon phase) potentials, and $E_{HOR}^{eq} = 0$ and $E_{ORR}^{eq} = 1.23$ V are the equilibrium potentials of the respective half-cell reaction. We will assume that the anode is grounded $\phi_a = 0$ and, hence, ϕ_c is the cell voltage. Equations 5 and 6 are good approximations if the membrane potential Φ does not vary significantly in the y-direction. A well-humidified PEM would ensure just that.

By substituting Eqs. 3–6 into Eq. 2 and introducing the dimensionless variables

$$\tilde{x} = \frac{x}{l_m}, \quad \tilde{j} = \frac{j l_m}{\sigma_m b_{ox}}, \quad \tilde{\Phi} = \frac{\Phi}{b_{ox}}, \quad \tilde{\phi} = \frac{\phi}{b_{ox}}, \quad \tilde{b}_{hy} = \frac{b_{hy}}{b_{ox}}, \quad [7]$$

we arrive at

$$\frac{d^2 \tilde{\Phi}}{d\tilde{x}^2} = 2\tilde{j}_{ox}^{\infty} \sinh\left(-\tilde{\phi}_c + \tilde{\Phi} + \tilde{E}_{ORR}^{eq}\right) - 2\tilde{j}_{hy} \sinh\left(-\tilde{\Phi}/\tilde{b}_{hy}\right). \quad [8]$$

Here, $\tilde{j}_{ox}^{\infty}$ is equipped with the superscript ∞ to indicate that this parameter is independent of $\tilde{x}$.

In the anode-free domain, $\tilde{x} < 0$, the anode exchange current density vanishes. For $\tilde{j}_{hy}$, we therefore have

$$\tilde{j}_{hy} = \tilde{j}_{hy}^{\infty} H(\tilde{x}), \quad [9]$$

where $\tilde{j}_{hy}^{\infty}$ is the HOR exchange current density in the working domain and H is the Heaviside step function: $H(\tilde{x}) = 0$ for $\tilde{x} < 0$ and $H(\tilde{x}) = 1$ for $\tilde{x} \geq 0$.

We will assume that the cell voltage ϕ_c is fixed; the respective mean cell current density $\tilde{J}$ can be calculated from the equation $\tilde{J} = 2\tilde{j}_{hy}^{\infty} \sinh(-\tilde{\Phi}^{\infty}/\tilde{b}_{hy})$. The value of $\tilde{\Phi}^{\infty}$ is a solution to Eq. 15, as discussed below.

Analytical Solution

Anode-free domain ($\tilde{x} < 0$).— In the anode-free area, the anode current density $\tilde{j}_a$ vanishes and Eq. 8 simplifies to

$$\frac{d^2\tilde{\Phi}}{d\tilde{x}^2} = 2\tilde{j}_{ox}^{\infty} \sinh\left(-\tilde{\phi}_c + \tilde{\Phi} + \tilde{E}_{ORR}^{eq}\right). \quad [10]$$

It is convenient to rewrite Eq. 10 in terms of the cathode overpotential, defined in Eq. 6, which reads in dimensionless form

$$\tilde{\eta}_c = \tilde{\phi}_c - \tilde{\Phi} - \tilde{E}_{ORR}^{eq}. \quad [11]$$

With this in mind, Eq. 10 transforms to

$$\frac{d^2\tilde{\eta}_c}{d\tilde{x}^2} = 2\tilde{j}_{ox}^{\infty} \sinh(\tilde{\eta}_c) \quad \text{with} \quad \tilde{\eta}_c(0) = \tilde{\eta}_c^0, \quad \tilde{\eta}_c(-\infty) = 0. \quad [12]$$

Here, the boundary conditions fix the cathode overpotential at the anode edge ($\tilde{x} = 0$) and prescribe zero overpotential at $\tilde{x} \to -\infty$, where the cathode current $\tilde{j}_c$ is zero.

Formally, the problem (12) is analogous to the Gouy–Chapman problem for the potential distribution inside the diffuse double layer at an infinite, flat metal/electrolyte interface. Here, the "metal" part of the domain is represented by the working domain of the cell ($\tilde{x} \geq 0$), while the "electrolyte" part is represented by the anode-free domain ($\tilde{x} < 0$).

The solution to Eq. 12 can be obtained by use of the procedure described in Ref. 14 (page 547):

$$\tilde{\eta}_c^-(\tilde{x}) = 2 \ln\left(\frac{1 - B \exp\left(\sqrt{2\tilde{j}_{ox}^{\infty}}\, \tilde{x}\right)}{1 + B \exp\left(\sqrt{2\tilde{j}_{ox}^{\infty}}\, \tilde{x}\right)}\right), \quad \tilde{x} \leq 0, \quad [13]$$

where the superscript "−" refers to the domain $\tilde{x} < 0$. Equation 13 obviously satisfies the boundary condition at $\tilde{x} = -\infty$. The constant B in Eq. 13 is obtained from a matching conditions (Matching procedure section).

Working domain.— In the working domain, $\tilde{x} > 0$, Eq. 8 can be re-written as

$$\frac{d^2\tilde{\Phi}}{d\tilde{x}^2} = 2\tilde{j}_{ox}^{\infty} \sinh\left(\tilde{\Phi} + \tilde{E}_{ORR}^{eq} - \tilde{\phi}_c\right) + 2\tilde{j}_{hy}^{\infty} \sinh\left(\frac{\tilde{\Phi}}{\tilde{b}_{hy}}\right). \quad [14]$$

Far from the anode edge inside the working domain, meaning $\tilde{x} \to \infty$, the right side vanishes since the anode and cathode current densities balance. The reason is that the boundary effects, stemming from the anode edge, are no longer felt. This defines the membrane potential at infinity

$$\tilde{\Phi}^{\infty} = \tilde{\Phi}(\tilde{x} \to \infty),$$

which is a solution to the equation

$$2\tilde{j}_{ox}^{\infty} \sinh\left(\tilde{\Phi}^{\infty} + \tilde{E}_{ORR}^{eq} - \tilde{\phi}_c\right) + 2\tilde{j}_{hy}^{\infty} \sinh\left(\frac{\tilde{\Phi}^{\infty}}{\tilde{b}_{hy}}\right) = 0. \quad [15]$$

In turn, the potential $\tilde{\Phi}^{\infty}$ defines the overpotentials, Eqs. 5 and 6, at a large distance ($\tilde{x} \gg 1$) from the anode edge.

Owing to the large exchange current density of the HOR, even a small variation in $\tilde{\Phi}$ strongly changes the HOR rate in the ACL. Thus, as we approach the anode edge from a position far inside the working domain, a small deviation of $\tilde{\Phi}$ from $\tilde{\Phi}^{\infty}$ leads to a significant imbalance in anode and cathode current densities. We attempt to capture

this behavior by expressing the solution as $\tilde{\Phi} = \tilde{\Phi}^{\infty} + \tilde{\Phi}^1$, where $\tilde{\Phi}^1$ is small. Substitution into Eq. 14 and expansion of the right side of this equation up to first order in $\tilde{\Phi}^1$ yields

$$\frac{d^2\tilde{\Phi}^1}{d\tilde{x}^2} = m^2 \tilde{\Phi}^1 \quad \text{with} \quad \tilde{\Phi}^1(\infty) = 0 \quad [16]$$

and

$$m = \sqrt{2\tilde{j}_{ox}^{\infty} \cosh\left(\tilde{\Phi}^{\infty} + \tilde{E}_{ORR}^{eq} - \tilde{\phi}_c\right) + \frac{2\tilde{j}_{hy}^{\infty}}{\tilde{b}_{hy}} \cosh\left(\frac{\tilde{\Phi}^{\infty}}{\tilde{b}_{hy}}\right)}. \quad [17]$$

The solution of the problem (16) is a simple exponential function. Therefore, we find for the membrane potential in the working domain

$$\tilde{\Phi}^+(\tilde{x}) = \tilde{\Phi}^{\infty} - \xi e^{-m\tilde{x}}, \quad \tilde{x} \geq 0. \quad [18]$$

In terms of the overpotential, this reads

$$\tilde{\eta}_c^+(\tilde{x}) = \tilde{\eta}_c^{\infty} + \xi e^{-m\tilde{x}}, \quad [19]$$

where m is given by Eq. 17 and

$$\tilde{\eta}_c^{\infty} = \tilde{\phi}_c - \tilde{\Phi}^{\infty} - \tilde{E}_{ORR}^{eq} \quad [20]$$

is the cathode overpotential in the working domain at a large positive distance from the anode edge. Below, we will see that $\tilde{\eta}_c \approx \tilde{\eta}_c^{\infty}$ already holds at $\tilde{x} \gtrsim 1$.

The parameter ξ in Eqs. 18 and 19 is a constant to be determined by matching conditions (see below). The superscript "+" denotes the solution for $\tilde{x} \geq 0$, and $\tilde{\Phi}^{\infty}$ is a solution to Eq. 15. Importantly, the small magnitude of $\tilde{\Phi}^1$ is explained by the large value of the HOR exchange current density, as discussed above. In non-hydrogen fuel cells or in SOFCs, $\tilde{\Phi}^1$ may not be small and the procedure, which leads to Eq. 18, may not be valid. In this case, a simple expansion of the right side of Eq. 14 up to second order may yield a more accurate picture but it does not allow for an analytical solution. Instead, it is advisable to obtain a numerical solution to the full problem, represented by Eq. 8, and check the magnitude of $|\tilde{\Phi}(0) - \tilde{\Phi}^{\infty}|$. This helps gauge whether a linearization is justified or not.

It should be emphasized, however, that *the characteristic length scale* of the $\tilde{\Phi}$ and $\tilde{\eta}^-$ variation inside the anode-free domain, embedded in Eq. 13, remains the same regardless of the value of $\tilde{\Phi}^1$; only the constant B is affected by the matching procedure discussed below. For the results in Placing the Reference Electrode section it is important that the characteristic scale of the $\tilde{\eta}^-$ variation in Eq. 13 is independent of B.

Matching procedure.— The parameters B and ξ are determined by the continuity of $\tilde{\eta}_c$ and $d\tilde{\eta}_c/d\tilde{x}$ at $\tilde{x} = 0$. Equating the overpotential functions (13) and (19) at $\tilde{x} = 0$, and equating their derivatives at this point, we derive a system of two equations

$$2 \ln\left(\frac{1 - B}{1 + B}\right) = \tilde{\eta}_c^{\infty} + \xi,$$

$$-\frac{4B\sqrt{2\tilde{j}_{ox}^{\infty}}}{1 - B^2} = -m\xi.$$

By eliminating ξ, this reduces to a single equation for B:

$$2 \ln\left(\frac{1 - B}{1 + B}\right) = \tilde{\eta}_c^{\infty} + \frac{4B\sqrt{2\tilde{j}_{ox}^{\infty}}}{m(1 - B^2)}. \quad [21]$$

Note that the left side of Eq. 21 must be negative since $\tilde{\eta}_c$ is negative. This means that $0 < B < 1$. The solution to Eq. 21 fully determines the shape of the cathode overpotential and its related system characteristics along the whole axis $\tilde{x}$. A simple procedure for the numerical solution of Eq. 21 is described in Appendix.

Peak of the anode current density.— An interesting feature of the solution above, which is specific to PEMFCs, is a large peak of the anode current density in the vicinity of the anode edge. The value of

Table I. The physical parameters for the calculations.

ORR exchange current density j_{ox}^∞, A cm^{-2}	10^{-6}
ORR equilibrium potential E_{ORR}^{eq}, V	1.23
ORR Tafel slope b_{ox}, V	0.03
HOR exchange current density in the working domain j_{hy}^∞, A cm^{-2}	1.0
HOR Tafel slope b_{hy}, V	0.015
Membrane proton conductivity σ_m, Ω^{-1} cm^{-1}	0.1
Membrane thickness l_m, cm	0.0025 (25 μm)
Cell voltage ϕ_c, V	0.83446
Mean current density in the working domain J, A cm^{-2}	1

this peak is given by $\tilde{j}_a^{peak} = 2\tilde{j}_{hy}^\infty \sinh(-\tilde{\Phi}(0)/\tilde{b}_{hy})$. With Eqs. 11 and 13, we find

$$\tilde{j}_a^{peak} = 2\tilde{j}_{hy}^\infty \sinh\left(\frac{\tilde{E}_{ORR}^{eq} - \tilde{\phi}_c}{\tilde{b}_{hy}} + \frac{2}{\tilde{b}_{hy}} \ln\left(\frac{1-B}{1+B} \right) \right), \qquad [22]$$

where B is the solution to Eq. 21.

From the exponential behavior of $\tilde{\Phi}$ at $\tilde{x} > 0$, given by Eq. 18, it follows that the non–dimensional characteristic width $\tilde{l}_{peak}$ of the anode current peak is $1/m$. With m given by Eq. 17, we find

$$\tilde{l}_{peak} = \left[2\tilde{j}_{ox}^\infty \cosh\left(\tilde{\Phi}^\infty + \tilde{E}_{ORR}^{eq} - \tilde{\phi}_c \right) + \frac{2\tilde{j}_{hy}^\infty}{\tilde{b}_{hy}} \cosh\left(\frac{\tilde{\Phi}^\infty}{\tilde{b}_{hy}} \right) \right]^{-1/2}. \qquad [23]$$

When all the parameter values are fixed, this is a function of $\tilde{\phi}_c$ (or, equivalently, of the mean current density $\tilde{J}$) since $\tilde{\Phi}^\infty$ depends on $\tilde{\phi}_c$ via Eq. 15.

In dimensional form, Eq. 23 reads

$$l_{peak} = l_m \left[2\tilde{j}_{ox}^\infty \cosh\left(\tilde{\Phi}^\infty + \tilde{E}_{ORR}^{eq} - \tilde{\phi}_c \right) + \frac{2\tilde{j}_{hy}^\infty}{\tilde{b}_{hy}} \cosh\left(\frac{\tilde{\Phi}^\infty}{\tilde{b}_{hy}} \right) \right]^{-1/2}. \qquad [24]$$

At sufficiently large cell current densities, the cosh-functions in Eq. 24 can be replaced by one half times the leading-order exponential term of each cosh-function. In this case, the first term in the square brackets in Eq. 24 equals $\tilde{J}$ while the second term is $\tilde{J}/\tilde{b}_{hy}$. Hence, we obtain

$$l_{peak} \simeq \sqrt{\frac{\sigma_m b_{ox} l_m}{J(1 + b_{ox}/b_{hy})}} \simeq \sqrt{\frac{\sigma_m b_{ox} l_m}{3J}}. \qquad [25]$$

Here, the last equation is based on the estimate $b_{ox} \simeq 2b_{hy}$ (see Table I).

The shapes of the potentials and current densities are shown in Fig. 4. For a cell current density of 1 A cm^{-2}, the peak anode current density j_a^{peak} is 3.96 A cm^{-2}; the dependence of j_a^{peak} on the cell current density J is depicted in Fig. 5.

Note also a very slow decay of the magnitude of the cathode overpotential η_c as $\tilde{x} \to -\infty$ (Fig. 4a). This decay is of particular interest for the proper placing of the reference electrode, as discussed in the next section.

Placing the Reference Electrode

Characteristic scale of the decay in membrane potential as $\tilde{x} \to -\infty$.— The $\tilde{\Phi}$ variation along $\tilde{x}$ contains two spatial scales. The first characteristic length is $\tilde{l}_{peak} = l_{peak}/l_m$ (see Eq. 24). It determines the exponential shape of $\tilde{\Phi}$ at $\tilde{x} > 0$, as discussed in the previous section. Another scale, denoted by $\tilde{l}_*$, determines the exponential–like variation of $\tilde{\Phi}$ inside the anode-free domain, $\tilde{x} < 0$. From Eq. 13 it follows that this scale is given by $\tilde{l}_* = 1/\sqrt{2\tilde{j}_{ox}^\infty}$. In dimensional form, this equation reads

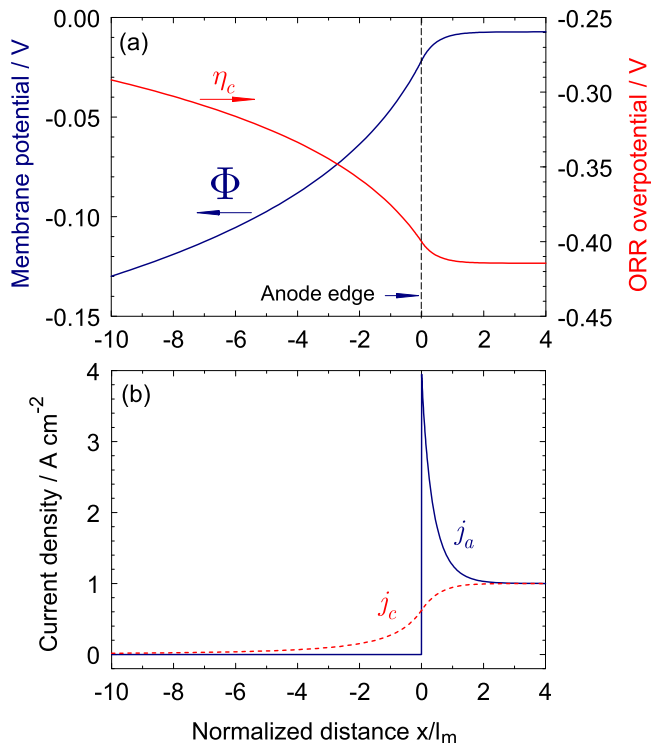$$l_* = \sqrt{\frac{\sigma_m b_{ox} l_m}{2 j_{ox}^\infty}}. \qquad [26]$$

Figure 4. Potentials and currents near the single anode edge (see Fig. 3 for the geometry of the problem). (a) The shapes of the membrane potential Φ and the ORR overpotential η_c; (b) cathode (j_c) and anode (j_a) current densities.

Thus, a convergence of $\Phi(x)$ toward the limiting value, which corresponds to a vanishing cathode current inside the anode-free domain, occurs at a distance L_{gap} on the order of $3l_*$ from the anode edge (Fig. 6). Here, the factor 3 is taken to ensure a complete convergence. With the data from Table I, we find $L_{gap} \simeq 6$ cm. Note, however, that this estimate implies a fully humidified state of the membrane. According to (26), the length l_* can be decreased by lowering the membrane conductivity σ_m or by increasing the amount of catalyst in the CCL to increase j_{ox}^∞.

Reference electrode potential.— Consider a system with the reference electrode located at a distance $L_{gap} \simeq 3l_*$ from the edge of the working anode (Fig. 7a). Suppose that the working anode is grounded, the RE is supplied with hydrogen and only a small current, which is
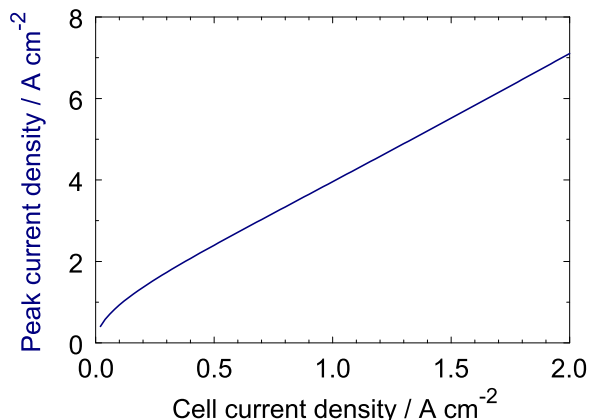

Figure 5. Peak current density at the edge of the anode as a function of the cell current density. Parameters for the calculation are listed in Table I.
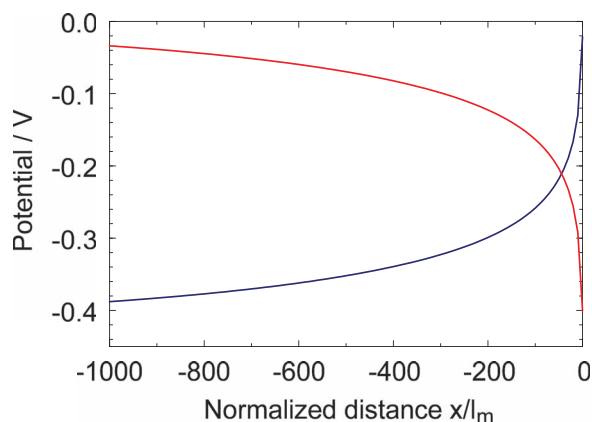
Figure 6. The membrane potential Φ and the cathode overpotential η_c in the anode–free domain (Fig. 3). The edge of the working anode is located at $\tilde{x} = 0$. For the parameters in Table I, $l_* \simeq 2$ cm.
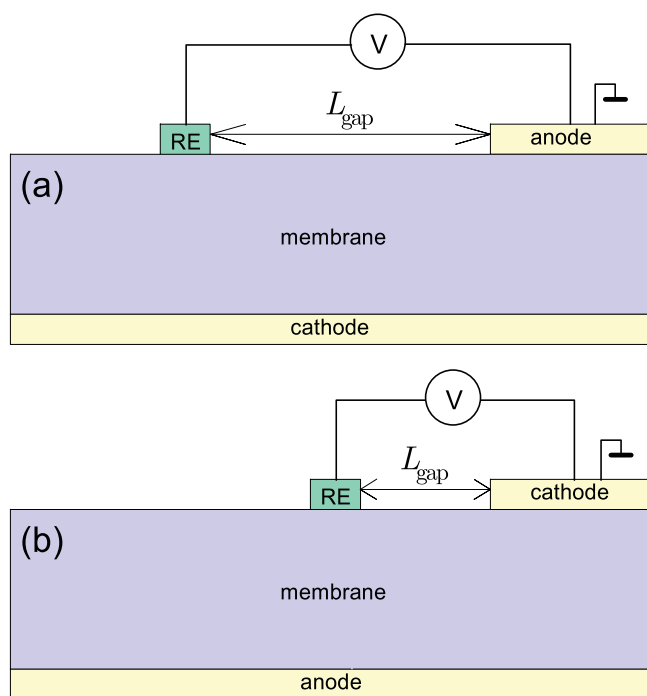

Figure 7. (Not to scale) (a) Schematic of PEM fuel cell electrodes with the reference electrode (RE) at a distance L_{gap} from the working anode edge. (b) The system with swapped anode and cathode. The potential of the RE is now related to the working anode overpotential. Note the much smaller distance L_{gap} (see text for discussion).

required to measure the RE potential, runs through this electrode.[d] In this case, the potential loss for the HOR activation in the RE, and all the resistive losses between the RE and the working anode, can be safely ignored. Then, the potential drop between the RE and the working anode is equal to the cathode overpotential η_c^∞ *in the working domain* (Fig. 7a).

To show this, we write Eq. 6 for $\tilde{x} \to -\infty$ and for $\tilde{x} \to \infty$:

$$\eta_c^{-\infty} = \phi_c - \Phi^{-\infty} - E_{ORR}^{eq} = 0, \qquad [27]$$

$$\eta_c^\infty = \phi_c - \Phi^\infty - E_{ORR}^{eq}. \qquad [28]$$

Solving Eq. 27 for ϕ_c and substituting the result into Eq. 28, we obtain

$$\eta_c^\infty = \Phi^{-\infty} - \Phi^\infty \simeq \Phi^{-\infty}, \qquad [29]$$

where we used $\Phi^\infty \simeq 0$ (Fig. 4a). The validity of Eq. 29 is further supported by simple inspection of Fig. 6. Further, at vanishingly small currents in the hydrogen-fed RE, the potential of this electrode is roughly $\phi_{ref} \simeq \Phi^{-\infty}$. With Eq. 29, we finally find $\phi_{ref} \simeq \eta_c^\infty$ (Fig. 6).

Discussion

The key issue for the reference electrode system, depicted in Fig. 7a, is the characteristic scale l_* of the overpotential variation in the electrode-free domain ($x < 0$ in Fig. 3). Once again we stress that the large-scale parameter l_* is independent of the constant B, which appears in Eq. 13. In other words, l_* does not depend on the small-scale details of the $\tilde{\eta}$ variation in the vicinity of the working electrode's (anode) edge. Thus, the solution for the "remote" region in the anode-free domain ($\tilde{x} < 0, |\tilde{x}| \gg 1$) and the schematic in Fig. 7a are applicable to any type of fuel cell. However, in fuel cells other than PEMFC or HT–PEMFC, the potential Φ^∞ cannot be neglected and from Eq. 29 we find

$$\phi_{ref} = \eta_c^\infty + \Phi^\infty. \qquad [30]$$

This means that the RE measures the sum of the working cathode overpotential and the membrane potential between the working electrodes.

The only value specific to the particular type of fuel cell, is the value of $L_{gap} = 3l_*$ (see Eq. 26). This is determined by the characteristic transport and kinetic parameters of the cell/electrode of interest. Note that Fig. 6 exhibits an important aspect for PEMFCs: with $L_{gap} \gtrsim l_* \simeq 2$ cm, we have $\Phi(-L_{gap}) \simeq \eta^\infty$ so that the requirement $L_{gap} \gg 3l_*$ could be redundant.

The three-electrode system depicted in Fig. 7a, has two advantages over the systems depicted in Fig. 1. Firstly, it eliminates the problem of misalignment of the working electrodes: the system in Fig. 7a has no edge on the cathode side, which greatly simplifies the system design and makes the interpretation of measurements more reliable. Secondly, in PEMFCs equipped with this system, the potential of the reference electrode equals the overpotential of the cathode. The only drawback of the system in Fig. 7a is the large distance L_{gap} between the working and reference electrodes.

Finally, consider a system with a swapped anode and cathode (Fig. 7b). In this case, the distance L_{gap} is three orders of magnitude smaller as compared to Fig. 7a. Indeed, for the design in Fig. 7b, Eq. 26 takes the form

$$l_{**} = \sqrt{\frac{\sigma_m b_{hy} l_m}{2 j_{hy}^\infty}} \qquad [31]$$

with j_{hy}^∞ in the denominator, which is six orders of magnitude higher than j_{ox}^∞. For typical PEMFC parameters, $L_{gap} = 3l_{**}$ is on the order of 60 μm. For the RE potential in Fig. 7b we find

$$\phi_{ref} = \eta_a^\infty + \Phi^\infty. \qquad [32]$$

Here, both terms on the right side are small. This explains the failure of attempt[4] to measure the cathode overpotential, using a design similar to that in Fig. 2.

Conclusions

We report a model for a semi–infinite, straight-edge anode catalyst layer, facing a large-area (infinite) cathode catalyst layer in a PEM fuel cell. An analytical treatment of this problem yields a simple relation

for the characteristic length l_* of the exponential-like variation of the membrane potential in the anode-free domain. From this solution, it follows that a hydrogen-fed reference electrode, placed at a distance $3l_*$ from the edge of a working anode, has a potential which coincides with the cathode overpotential in the working domain of the cell. For typical PEMFC parameters, l_* is about 2 cm; however, this value can be reduced by increasing the catalyst loading on the cathode side.

Appendix: Numerical Solution to Eq. 21

The numerical solution to Eq. 21 can be obtained, using the following iterative procedure. First, we introduce $\varepsilon = 1 - B$. Clearly, as $0 < B < 1$, we have $0 < \varepsilon < 1$. Substituting $\varepsilon = 1 - B$ into Eq. 21 and solving this equation for ε *appearing inside the logarithm*, we arrive at an iterative scheme

$$\varepsilon_{n+1} = 2 \left[1 + \exp\left(\frac{\tilde{\eta}_c^\infty}{2} - \frac{2(1-\varepsilon_n)\sqrt{2\tilde{j}_{ox}^\infty}}{m\varepsilon_n(2-\varepsilon_n)} \right) \right]^{-1}.$$

The initial guess for iterations can be any number between 0 and 1, e.g., $\varepsilon_0 = 0.5$. Ten iterations provide five to six significant digits in the result. The parameter B is then restored as $B = 1 - \varepsilon_9$.

List of Symbols

~	Marks dimensionless variables
b	Tafel slope (V)
E^{eq}	Equilibrium half-cell potential (V)
F	Faraday constant
J	Mean current density in the working domain (A cm^{-2})
j_a	Local proton current density at the anode side (A cm^{-2})
j_c	Local proton current density at the cathode side (A cm^{-2})
j_{hy}	HOR exchange current density (A cm^{-2})
j_{hy}^∞	HOR exchange current density in the working domain (A cm^{-2})
j_{ox}^∞	ORR exchange current density (A cm^{-2})
L_{gap}	Gap length between the edge of the working electrode and the reference electrode
l_m	Membrane thickness (cm)
l_*	Characteristic length of Φ variation in the anode-free domain (cm)
R	Gas constant
x	Coordinate along the membrane (cm)
y	Coordinate through the membrane (cm)

Greek

η	Local overpotential (V)
σ_m	Membrane ionic conductivity (Ω^{-1} cm^{-1})
Φ	Membrane potential (V)
ϕ	Carbon phase (electrode) potential (V)
ϕ_{ref}	Carbon phase potential of the reference electrode

Subscripts

a	Anode
c	Cathode
HOR	Hydrogen oxidation reaction
hy	Hydrogen
m	Membrane
ORR	Oxygen reduction reaction
ox	Oxygen
ref	Reference electrode

Superscripts

∞	Working domain
0	at the edge of the working anode ($\tilde{x} = 0$)
1	Small perturbation

References

1. J. Giner, *J. Electrochem. Soc.* **111**, 376 (1964).
2. A. C. West and J. Newman, *J. Electrochem. Soc.* **136**, 3755 (1989).
3. H. Kuhn, B. Andreaus, A. Wokaun, and G. G. Scherer, *Electrochimica Acta* **51**, 1622 (2006).
4. J. H. Ohs, U. Sauter, S. Maass, and D. Stolten, *J. Electrochem. Soc.* **159**, F181 (2012).
5. S. B. Adler, B. T. Henderson, M. A. Wilson, D. M. Taylor, and R. E. Richards, *Solid State Ionics* **134**, 35 (2000).
6. J. Winkler, P. V. Hendriksen, N. Bonanos, and M. Mogensen, *J. Electrochem. Soc.* **145**, 1184 (1998).
7. S. B. Adler, *J. Electrochem. Soc.* **149**, E166 (2002).
8. D. Gerteisen, *J. Appl. Electrochem.* **37**, 1447 (2007).
9. J. Rutman and I. Riess, *Electrochimica Acta* **52**, 6073 (2007).
10. W. He and T. V. Nguyen, *J. Electrochem. Soc.* **151**, A185 (2004).
11. S. Almheiri and H. Liu, *J. Power Sources* **246**, 899 (2014).
12. A. A. Kulikovsky and P. Berg, *ECS Electrochem. Lett.* **9**, F64 (2013).
13. A. A. Kulikovsky, *SIAM J. Appl. Math.* **70**, 531 (2009).
14. A. J. Bard and L. R. Faulkner, *Electrochemical Methods. Fundamentals and Applications*, Wiley, New-York, 2001.